Analysis of the $J^P = 1^+$ and 0^- three-pion systems

R. Aaron
Department of Physics, Northeastern University, Boston, Massachusetts 02115

R. S. Longacre
Brookhaven National Laboratory, Upton, New York 11973
(Received 7 November 1980)

We analyze 3π production results obtained from recent diffractive and charge-exchange experiments. We find that two resonances, a $J^P = 1^+$ (A_1) and a $J^P = 0^-$ (π') are required by the data. The resonance parameters are $M_{A_1} = 1230 \pm 30$ MeV, $\Gamma_{A_1} = 350 \pm 60$ MeV, and $M_{\pi'} = 1273 \pm 50$ MeV, $\Gamma_{\pi'} = 580 \pm 100$ MeV. We interpret the above resonances in terms of $q\bar{q}$ and $q^2\bar{q}^2$ quark-model states.

I. INTRODUCTION

Recent high-statistics experiments involving the diffractive reaction $\pi^- p \to (3\pi)p$ (Ref. 1), and the charge-exchange reaction $\pi^- p \to (3\pi)n$ (Ref. 2) shed new light on the A_1 problem. Amplitude analysis of the $\rho\pi$ diffractive data indicates a peak in the $J^P = 1^+$ cross section, and large and rapid variation of the associated phase, near 1300 MeV. An Aitchison-Bowler analysis[3] yields the A_1 parameters $M_{A_1} = 1280 \pm 30$ MeV, $\Gamma_{A_1} = 300 \pm 30$ MeV.[1] The charge-exchange results are less definitive, but we show that they imply an A_1 consistent with that obtained from the diffractive data.

In the present paper we analyze the ACCMOR and CEX results including $\rho\pi$ *and* $\epsilon\pi$ production, using a generalized version of the Aitchison-Bowler techniques mentioned earlier. The resulting width of the A_1 into $\epsilon\pi$ is surprisingly small, and as a result, our A_1 parameters are very similar to those of ACCMOR who considered only $\rho\pi$. Our principal new result is the existence of a $J^P = 0^-$ resonance (π') with parameters $M_{\pi'} = 1273 \pm 50$ MeV with $\Gamma_{\pi'} = 508 \pm 100$ MeV. The corresponding A_1 parameters are $\Gamma_{A_1} = 1230 \pm 30$ MeV and $\Gamma_{A_1} = 350 \pm 60$ MeV. In Sec. II we define our basic isobar formalism, and discuss the partial-wave analysis of the isobar amplitudes.

A major obstacle to accurate theoretical analysis of the A_1 in strong-interaction experiments is its production in the presence of large nonresonant, Deck-type backgrounds which have rapid variation within the A_1 width. Moreover, analysis indicates that, when produced, the 1^+ $\rho\pi$ system behaves like resonance *plus* background, rather than pure resonance. In our model the effective 1^+ background is generated by a higher-mass A_1. Since our final A_1 parameters are very similar to those of ACCMOR who fit the 1^+ $\rho\pi$ data with a "single" A_1, one must conclude that the diffractive production of the resonant term which acts as a background is small. We show that this is the case in Sec. V. It is clear that a detailed dynamical theory is required to explain such complicated phenomena. However, no such theory exists, and we believe that the next best approach is a phenomenological framework which takes into account important principles such as unitarity and analyticity. For these purposes, we find the type of model first proposed by Aitchison and Bowler[3] to be most satisfactory. In Sec. III we derive a multichannel generalization of the latter work for application to the 1^+ and 0^- $\rho\pi$ and $\epsilon\pi$ systems.

The details of our fitting procedures are discussed in Sec. IV, and results and conclusions are given in Secs. V and VI, respectively. In the latter section we speculate that a four-quark ($q^2\bar{q}^2$) state proposed by Jaffe[4] is responsible for the observed "nonresonant" background in the A_1 channel.

Finally, in the main text, we try to avoid complicated derivations which interrupt the logical flow of ideas; such necessary discussions and derivations appear, rather, in Appendices A and B.

II. CROSS SECTIONS AND PARTIAL-WAVE ANALYSIS

We develop an isobar model to study the three-pion systems produced in the diffractive reaction $\pi^- + p \to (3\pi) + p$, and the charge-exchange reaction $\pi^- + p \to (3\pi) + n$. We shall assume that the diffractive reaction proceeds entirely through Pomeron (P) exchange, while the CEX reaction goes solely via ρ exchange. Both Pomeron and ρ exchanges are natural-parity exchanges. In general we shall label the 3 amplitudes by M^η, where M is the magnitude of the z component of the angular momentum in the Gottfried-Jackson frame,[5] and η is the exchange parity (+ for natural, and − for unnatural). Both the Pomeron and ρ can excite $M = 1$ and $M = 0$. The $M = 1$ amplitudes are small for the

 © 1981 The American Physical Society

Pomeron and we shall ignore them.

Assuming that the three final-state pions are produced exclusively in the particle-isobar combinations $\rho\pi$ and $\epsilon\pi$, we thus define a pseudo-T-matrix element describing three-pion production,

$$\langle k_1\tau_1, k_2\tau_2, k_3\tau_3 | T(W_A) | \alpha\rangle = T_{\epsilon\alpha} + T_{\rho\alpha} \tag{2.1}$$

with the isobar decompositions

$$T_{\epsilon\alpha} = \frac{1}{(3!)^{1/2}} \sum_{i,j,k\,(\text{cyclic})} \langle k_i | f_{\epsilon\alpha}(W_A) | \alpha\rangle e^{i\delta_\epsilon} \sin\delta_\epsilon \frac{\omega_\epsilon}{q_\epsilon} \langle t_i t_\epsilon \tau_i \tau_\epsilon | 1\tau_\pi\rangle \langle t_j t_k \tau_j \tau_k | t_\epsilon \tau_\epsilon\rangle , \tag{2.2}$$

$$T_{\rho\alpha} = \frac{1}{(3!)^{1/2}} \sum_{\substack{i,j,k\,(\text{cyclic})\\ \lambda}} \langle k_i \lambda | f_{\rho\alpha}(W_A) | \alpha\rangle e^{i\delta_\rho} \sin\delta_\rho \frac{\sqrt{3}\omega_\rho}{q_\rho^3} (V_{jk})_\lambda \langle t_i t_\rho \tau_i \tau_\rho | 1\tau\rangle \langle t_j t_k \tau_j \tau_k | t_\rho \tau_\rho\rangle . \tag{2.3}$$

In Eq. (2.1), $\alpha = P$ or ρ and $|\alpha\rangle$ represents either a πP or $\pi\rho$ initial state corresponding to a particular M^η; W_A is the 3π c.m. energy, the k_i's are the final-state pion momenta, and the τ_i's are the corresponding third components of isospin. We refer to T in (2.1) as a *pseudo-T*-matrix because the P or ρ in the initial state are Regge exchanges rather than true particles.

In Eqs. (2.2) and (2.3) we are treating identical particles as in Ref. 6, hence the factors $1/(3!)^{-1/2}$. δ_ϵ and δ_ρ are the π-π phase shifts in the $I=0$, $J=0$ and $I=1$, $J=1$ states, respectively, with $\omega_\epsilon, q_\epsilon$ and ω_ρ, q_ρ the corresponding c.m. energies and momenta. In (2.3) $\vec{V}$ is an off-shell polarization vector, with $\vec{V}^2$ a Lorentz invariant and equal to the square of the c.m. momentum of the pions in the ρ (Ref. 6).

It is the matrix elements of f_ϵ and f_ρ that will be related to experiment, and are the subject of the remainder of this section. We now expand (2.2) and (2.3) in terms of partial-wave amplitudes which will contain the fitting parameters of the analysis, i.e.,

$$\langle \vec{q} | f_{\epsilon\alpha}(W_A) | \alpha\rangle = \sum_{\substack{JM\\ l_q m_q\\ l_\alpha m_\alpha}} \langle qJl_q | f_{\epsilon\alpha}(W_A) | kJl_\alpha\rangle Y_{l_q m_q}(\hat{q}) Y^*_{l_\alpha m_\alpha}(\hat{k}) \langle l_\alpha s_\alpha m_\alpha \sigma_\alpha | JM\rangle , \tag{2.4}$$

$$\langle \vec{q}\lambda | f_{\rho\alpha}(W_A) | \alpha\rangle = \sum \langle qJl_q | f_{\rho\alpha}(W_A) | kJl_\alpha\rangle Y_{l_q m_q}(\hat{q}) Y^*_{l_\alpha m_\alpha}(\hat{k}) \langle l_\alpha s_\alpha m_\alpha \sigma_\alpha | JM\rangle \langle l_q 1 m_q \lambda | JM\rangle , \tag{2.5}$$

where k is the relative momentum in the initial state, and s_α is equal to zero for the Pomeron, and to one for the ρ. In Eqs. (2.2)–(2.5) we have adopted the following conventions in the Clebsch-Gordan coefficients (CGC's): (1) The pion always appears in the first position. (2) When coupling a particle and an isobar, the particle appears in the first position. (3) When coupling orbital angular momentum l and channel spin j, l appears in the first position. (4) In Eq. (2.3), for example, the particles in the isospin CGC appear in the same order as they do in the polarization vector $\vec{V}$.

Finally, following accepted procedures, we treat (2.1) as a standard T-matrix element, and express the cross section for three-pion production proceeding from an initial state $\alpha = \pi P$ or $\pi\rho$ with a particular M^η in the form

$$\sigma_\alpha(\tau_1, \tau_2, \tau_3) = \int d\rho^{(3)} |\langle k_1\tau_1, k_2\tau_2, k_3\tau_3 | T(W_A) | \alpha\rangle|^2 , \tag{2.6}$$

where the formula for n-body phase space is

$$d\rho^{(n)} = (2\pi)^4 \delta^4\left(P_f - \sum_{i=1}^n q_i\right) \prod_{i=1}^n (2\pi)^{-4} d^4 q_i 2\pi\delta^+(q_i^2 - m_i^2) . \tag{2.7}$$

We may express the above cross section in terms of the partial-wave amplitudes by substituting (2.4) and (2.5) into (2.6), obtaining

$$\sigma_\alpha(\tau_1, \tau_2, \tau_3) = \sum_{l, l_q} \int \frac{q^2 dq}{4(2\pi)^4} \left[|\langle qJl_q | f_{\epsilon\alpha}(W_A) | kJl\rangle|^2 \frac{\sin^2\delta_\epsilon(q)}{q} + |\langle qJl_q | f_{\rho\alpha}(W_A) | kJl\rangle|^2 \frac{\sin^2\delta_\rho(q)}{q^3}\right] + \text{cross terms} . \tag{2.8}$$

The above expressions can be compared directly with the published results of the various 3π partial-wave analyses. It is the *direct* terms and the phases of the partial-wave amplitudes that are quoted in the literature.

III. TWO-COMPONENT MODEL OF THE ISOBAR AMPLITUDES

A. Diffractive

We first develop a theoretical framework for diffractive 3π production which builds in what we

believe are the important reaction mechanisms and properties of the three-pion system:

(1) Diffractive production is simulated by assuming Pomeron exchange to be the only relevant mechanism. Thus all three-pion production proceeds from an initial pion-Pomeron (π-P) state.

(2) In our description of the Pomeron, it never appears in intermediate or final states of the 3π system.

(3) As explained in Appendix A, the quark structure of the three-pion system is included an isobar form by introducing the basic interactions

$$u_{ib}(q)(M_i - W_A - i\Gamma_i/2)^{-1}V_{iP}(p)\,, \tag{3.1}$$

$$u_{ib}(q)(M_i - W_A - i\Gamma_i/2)^{-1}u_{ia}(p)\,, \tag{3.2}$$

with

$$\Gamma_i = 2[u_{i\epsilon}(p_A)^2 + u_{i\rho}(p_A)^2]\,. \tag{3.3}$$

Equations (3.1) and (3.2) describe the reactions $\pi+P\to\pi+b$ and $\pi+a\to\pi+b$ ($a,b=\rho$ or ϵ), mediated by a particle of complex mass $M_i - i\Gamma_i/2$. The introduction of such particles is motivated by the known quark spectrum. In the $J^P=1^+$ three-pion system two such particles are introduced, related to the $q\bar{q}$ (~1100) and $q^2\bar{q}^2$ (~1250) described in Refs. 4 and 7.

The u_{ia} in (3.1) and (3.2) are taken as products of coupling constants and barrier factors, and their parametrization shall be discussed in Sec. IV. The vertex functions V_{iP} which describe coupling of the Pomeron, simulate diffractive production, and are much more complicated than the u_{ia}. Below we shall use unitarity to determine their optimum parametrization.

(4) Following the approach of Aitchison and Bowler,[3] we break the partial-wave amplitudes into two parts, the first describing 3π production via the Deck mechanism, and the second corresponding to direct coupling of the Pomeron to the 3π states suggested by the quark model. Thus using the notation of (2.4) and (2.5), we define

$$\langle qJl_q|\, f_{aP}(W_A)\,|p, J=l\rangle = f^D_{aP}(q,p;W_A) + f^R_{aP}(q,p;W_A)\,, \tag{3.4}$$

where f^D_{aP} is the Deck background and assumed to contain no iterations of the basic interactions (3.1) and (3.2), while f^R_{aP} describes resonance production and sums all diagrams in which $\epsilon\pi$ or $\rho\pi$ final states are produced by propagation and decay of one or another of the quark-related states discussed above. In (3.4) we have suppressed angular momentum labels on f^D and f^R, and shall continue to do so for the remainder of this section.

The Deck amplitudes f^D_{aP} are parametrized according to Ref. 8. The structure of the resonance amplitudes f^R_{aP} is determined by our model as explained in Appendix A. It is useful to define reduced amplitudes

$$\bar{f}_{aP} = \sqrt{\rho_a}\, f_{aP} \sqrt{\rho_P}\,, \tag{3.5}$$

which satisfy a modified unitarity relation (no phase-space factors)

$$\mathrm{Abs}\bar{f}_{aP}(s) = i\sum_b \bar{f}_{ab}(s)\bar{f}^*_{aP}(s), \quad s = W_A{}^2 \tag{3.6}$$

where

$$\mathrm{Abs}\bar{f}_{aP}(s) = [\bar{f}_{aP}(s+i\epsilon) - \bar{f}^*_{aP}(s-i\epsilon)]/2i\,. \tag{3.7}$$

It is important to note that $\mathrm{Abs}\bar{f}_{aP}$ is in general complex. In the traditional isobar model, $\mathrm{Abs}\bar{f}_{aP}$ would be real and equal to $\mathrm{Im}\bar{f}_{aP}$. This is not the case in (3.6) because the initial state contains a Pomeron which is not a normal particle. Corresponding to the reduced amplitudes $\bar{f}_{aP}$ appearing in (3.5) are reduced quantities $\bar{f}^D_{aP}$ and $\bar{f}^R_{aP}$ related to f^D_{aP} and f^R_{aP} of Eq. (3.4). In Appendix A we obtain the results

$$\bar{f}^R_{aP}(q,p;W_A) = \sum_{i,j=1}^{2} u_{ja}(q)D^{-1}_{\tilde{i}\tilde{j}}(W_A)V_{iP}(p)/\det|D|\,, \tag{3.8}$$

$$f^R_{ab}(q,p;W_A) = \sum_{i,j=1}^{2} u_{ja}(q)D^{-1}_{\tilde{i}\tilde{j}}(W_A)u_{ib}(p)/\det|D|\,, \tag{3.9}$$

where $\tilde{i}$ and $\tilde{j}$ are defined such that if $i=1$, then $\tilde{i}=2$, and vice versa.

$$D_{ii}(W_A) = M_i - W_A - i[u_{i\rho}{}^2(p_A) + u_{i\epsilon}{}^2(p_A)]\,, \tag{3.10}$$

$$D_{12}(W_A) = i[u_{1_\rho}(p_A)u_{2_\rho}(p_A) + u_{1\epsilon}(p_A)u_{2\epsilon}(p_A)]\,. \tag{3.11}$$

The zeros of $|D|$ in Eqs. (3.8) and (3.9) give the 3π resonant energies. In general D_{12} will, of course, have a real part, which is necessary to compare our amplitudes with those of Ref. 3. This comparison will be discussed in detail in a future publication by one of us (R.S.L.).

B. Charge exchange (CEX)

In the case of CEX we consider only the (nucleon) spin-flip data, which the partial-wave analysis shows to be dominated by natural-parity exchange. In line with this observation and theoretical estimates, we assume that the spin-flip 3π production reaction proceeds entirely through Reggeized ρ exchange. Thus in the 3π system we wish to study the reactions

$$\text{Reggeized } \rho+\pi \to \rho+\pi \text{ or } \epsilon+\pi\,. \tag{3.12}$$

If the initial state contained a real ρ rather than a Reggeized ρ, our formalism would provide very stringent mutual consistency constraints on the diffractive and CEX data, since the same ρ cou-

plings would be present in both. Such is not the case, however, and we thus make the following assumption concerning the Reggeon (ρ)-π-A vertex functions; namely, we write

$$Cu_{i\rho}(p) \tag{3.13}$$

in place of the $u_{i\rho}(p)$ appearing in (3.1), where C is a complex constant. This is the simplest choice consistent with analyticity, and the present state of theory and experiment does not seem to warrant a more sophisticated one.

IV. FITTING PROCEDURES

We have simultaneously fit the low-t [0.0–0.05 $(\mathrm{GeV}/c)^2$] and high-t [0.05–0.70 $(\mathrm{GeV}/c)^2$] partial-wave amplitudes obtained by ACCMOR,[1] along with the CEX[2] results. These fits involve parametrization of Eq. (3.4) and a subsequent χ^2 analysis. The total number of parameters involved in the fit to the diffractive amplitudes is 39, with 16 being used for the Deck contribution, and 21 to describe resonance production, propagation, and decay. In the diffractive case, the amplitude for $A_2 \to \rho\pi$ is taken as the reference. The overall phase of this amplitude is arbitrary, so two more fitting parameters enter our formalism to describe the variation of the latter phase from pure Breit-Wigner behavior at low t and at high t.

Only two additional parameters are required for the charge-exchange amplitudes. This is because we are considering specifically those CEX amplitudes corresponding to Reggeized ρ exchange and treating the incident Reggeon essentially as a normal s-channel $\pi\pi$ resonance. Thus the $\rho\pi$ production amplitude involves ordinary $\rho\pi$ scattering, which has already been parametrized for the diffractive data.

A. Diffractive data: Deck background

Our parametrization of the Deck part is that of Ref. 8; we choose

$$\bar{f}^D_{aP}(q,k;W_A) = \sqrt{\rho_a}\, B^{J^P}_{a,X} \exp(-\beta^{J^P}_{a,X} W_A)\,, \tag{4.1}$$

where ρ_a is two-body phase space given by (2.7). The 16 fitting parameters B and β are labeled by $a=\rho$ or ϵ, $J^P=1^+$ or 0^-, and $X=\mathrm{HT}$ or LT, where LT and HT refer to low t and high t, respectively.

B. Diffractive data: Resonance production

Parametrization of the resonant amplitudes $\bar{f}^R$ involves:

(1) Six parameters γ_{ia} appearing in the vertex functions u_{ia}

$$u_{i\rho}{}^2(q) = \frac{q}{\omega_q}\gamma_{i\rho}{}^2\,, \qquad u_{i\epsilon}{}^2(q) = \left(\frac{q}{\omega_q}\right)^3 \gamma_{i\epsilon}{}^2\,, \tag{4.2}$$

where for $J^P=1^+$, $i=1,2$, and $X=\mathrm{LT},\mathrm{HT}$, while for $J^P=0^-$, $i=2$, and $X=\mathrm{LT},\mathrm{HT}$. Note that in $J^P=0^-$ we are assuming only *one* quark-related state.

(2) Three mass parameters M_i ($i=1,2$ for $J^P=1^+$ and $i=2$ for $J^P=0^-$) appearing in the propagators in Eq. (3.10).

(3) Twelve real parameters (six complex parameters) are required for the Pomeron couplings V_{iP}. These are labeled by $X=\mathrm{LT},\mathrm{HT}$ with $i=1,2$ for $J^P=1^+$, and $i=2$ for $J^P=0^-$. The Pomeron couplings shall be discussed further below.

C. Structure of V_{iP}

It is important to note that V_{iP} appears linearly in (3.8) because in our formalism the Pomeron is assumed present only in the initial state. As pointed out earlier, it is a complex quantity which includes the effects of resonance production via direct coupling to the Pomeron as well as through Deck rescattering.

For phenomenological fitting it is useful to break up V_{iP} into dispersive and absorptive parts since it can be shown that $\mathrm{Abs}V_{iP}$ is directly proportional to the large and rapidly varying Deck backgrounds, and also that it includes threshold singularities in s.[9] On the other hand, $\mathrm{Disp}V_{iP}$ is a relatively smooth analytic function of s that can be parametrized with some confidence.[10]

We obtain the above breakup by substituting (3.4) and (3.5) into the modified unitarity relation (3.6) and using the explicit forms (3.8) and (3.9) for $\bar{f}^R_{aP}$ and $\bar{f}^R_{ab}$. These manipulations yield

$$\mathrm{Abs}V_{iP}(p_A) = \sum_a \bar{f}^D_{aP}(q_A,p_A;W_A)u_{ia}(q_A)\,. \tag{4.3}$$

In deriving (4.3) above we have used the fact that $\mathrm{Abs}(FG) = F^*\,\mathrm{Abs}(G) + G\,\mathrm{Abs}(F)$ *and assumed that* $\mathrm{Abs}f^D_a = 0$. The latter choice is made for simplicity, *and does not preclude* f^D_a *from being complex*. Having obtained $\mathrm{Abs}V_{iP}$, $\mathrm{Disp}V_{iP}$ is obtained from the identity

$$V_{iP} \equiv \mathrm{Disp}V_{iP} + i\,\mathrm{Abs}V_{iP}\,. \tag{4.4}$$

By using (4.3) we reduce the number of parameters needed for V_{iP} by 12, as well as taking into account explicitly the more singular part of V_{iP}.

D. Charge exchange

As discussed in Sec. IIIB, for CEX 3π production proceeding via (nucleon) spin-flip and Reggeized ρ

exchange, two real parameters (i.e., a single complex parameter C) enter our formalism. These parameters relate the Reggeon vertices to the normal-particle vertices, and also measure the relative normalization of the diffractive- and charge-exchange cross sections.

E. Extraction of 3π resonance parameters

In order to study 3π resonances we search for zeros of $\det|D|$ in Eq. (3.9). We rewrite (suppressing momentum and energy arguments)

$$f^R_{ab}=\frac{u_{1a}u_{1b}}{D_{11}}+\frac{(u_{2a}+D_{12}u_{1a}/D_{11})(u_{2b}+D_{12}u_{1b}/D_{11})}{D_{22}-D_{12}^2/D_{11}}\,. \tag{4.5}$$

Suppose that we are near a zero of $D_{22}-D_{12}^2/D_{11}$, and $u_{ia}u_{ib}/D_{11}$ is a slowly varying function which may be interpreted as nonresonant background. Such is the case in our fitted solutions. We then expand

$$D_{22}-\frac{D_{12}^2}{D_{11}}\approx M_A-W_A-i\frac{\Gamma_T}{2} \tag{4.6}$$

and interpret the 3π resonant mass M_A to be given by

$$\mathrm{Re}(D_{22}-D_{12}^2/D_{11})=0 \tag{4.7}$$

and the total width Γ_T as

$$\Gamma_T=-2\,\mathrm{Im}(D_{22}-D_{12}^2/D_{11})\,. \tag{4.8}$$

Equation (4.5) suggests the following definition of the partial widths Γ_a into $a\pi$:

$$\Gamma_a=|u_{2a}+D_{12}u_{1a}/D_{11}|^2\,. \tag{4.9}$$

With this definition, the total width Γ_T has the required form

$$\Gamma_T=\sum_{a=\rho,\epsilon}\Gamma_a\,. \tag{4.10}$$

V. RESULTS

Using Eq. (2.8) and the parametrizations discussed in Sec. IV, we now fit the results of the amplitude analyses of Refs. 1 and 2. We interpret each of the direct terms in (2.8) as a $\rho\pi$- or $\epsilon\pi$- production cross section with a given J^P, M^η, and l_q. The experimental results include just such $\rho\pi$ and $\epsilon\pi$ cross sections, and in addition, the phases of the partial-wave isobar amplitudes. There are 560 $J^P=1^+$ and 0^- diffractive data points, and 30 $J^P=1^+$ CEX points. The best fit within the theoretical framework described in the preceding text gives a χ^2 of 1214, with the CEX data contributing 59 to this value. In Figs. 1–8 we plot the diffractive cross sections and phases along with our best fit, and in Figs. 9 and 10 we

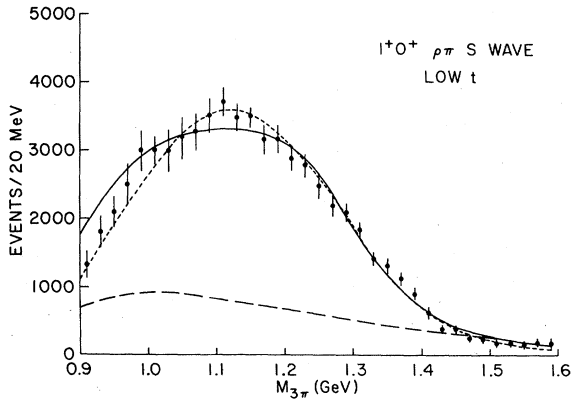

FIG. 1. LT, $J^PM^\eta=1^+0^+$ $\rho\pi$ s-wave cross sections without (solid curve) and with (short-dashed curve) rescattering corrections at low energies. The Deck contribution is shown separately (long-dashed curve).

do the same for the CEX data. We find that both a $J^P=1^+$ (A_1) and a $J^P=0^-$ (π') resonance are necessary to fit the data. The masses, widths, and partial widths of these resonances are displayed in Table I.

We shall now investigate important features of our solutions, determined by the behavior of χ^2.

(1) The π'. Since the π' is a newly discovered resonance, it is worth studying the sensitivity of χ^2 to the existence of this particle. In our model, the fit without a π' is very bad; $\chi^2=4262$. While it is absolutely clear that at least one π' must be introduced in order to explain the observed phase behavior in the 0^- waves, our actual resonance parameters must be taken with some reservation. The main reason is that for the case of the 0^- we have only considered the simplest form of our model (i.e., no 0^- background). A more sophisti-

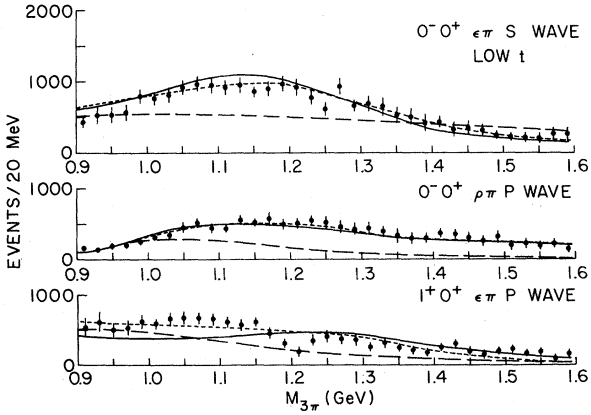

FIG. 2. LT, 1^+0^+ and 0^-0^+ $\rho\pi$ and $\epsilon\pi$ cross sections without (solid curve) and with (short-dashed curve) low-energy rescattering corrections. Deck contribution is shown separately (long-dashed curve).

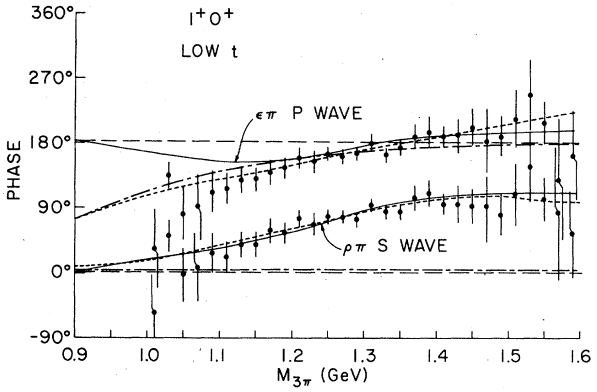

FIG. 3. LT, 1^+0^+ phases: (a) without rescattering (solid curve), (b) with rescattering (short-dashed curve), (c) Deck without rescattering (long-dashed curve), (d) Deck with rescattering (dot-dashed curve). The upper Deck curves are $\epsilon\pi$, and the lower ones are $\rho\pi$.

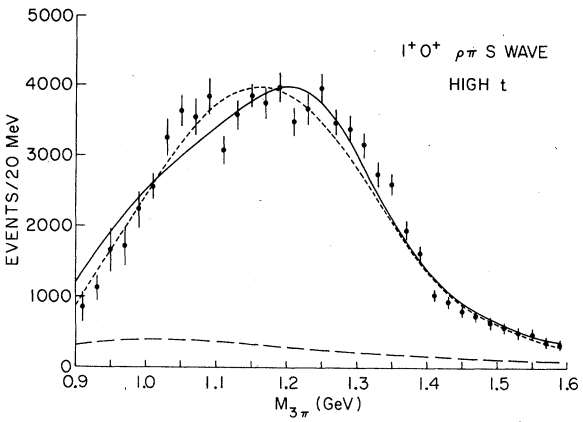

FIG. 5. HT, 1^+0^+ $\rho\pi$ s-wave cross sections.

cated background was required for the A_1 in order to obtain consistency with CEX data. The 0^- CEX data are still under investigation, and without these data it seems an unnecessary bother to include 0^- background in the present analysis.

(2) The $J^P=1^+$ background. In the absence of the CEX data we find acceptable fits to the data without a 1^+ background and with A_1 resonance parameters almost identical to those given in Ref. 1 (i.e., $M_{A_1} \approx 1280$ MeV, $\Gamma_{A_1} \approx 300$ MeV). However, the CEX data requires a background term. The reason is that the CEX 1^+ cross section peaks at 1130 MeV, and in a χ^2 sense, this behavior cannot be described satisfactorily with a single $J^P=1^+$ resonance term. With a resonance-background description, the CEX data points contribute 59 to the total χ^2; removing the background increases their contribution by 30. A key feature of the 1^+ background discussed above is that it is produced more strongly in the case of CEX than in diffraction. For example, consider the ratio

$$R=(\gamma_{1\rho}/\gamma_{2\rho})^2\text{diffractive}/(\gamma_{1\rho}/\gamma_{2\rho})^2\text{CEX}. \quad (5.1)$$

If we refer to the background as A_1^*, the quantities $(\gamma_{1\rho}/\gamma_{2\rho})^2$ are proportional to the cross-section ratio of A_1^* production to that of ordinary A_1 production. At low t we find

$$R_{\rm LT}=(80.6/84.6)^2/(2.02/0.980)^2=0.214 \quad (5.2)$$

and at high t,

$$R_{\rm HT}=(56.5/86.4)^2/(2.02/0.980)^2=0.101. \quad (5.3)$$

The above values for $R_{\rm LT}$ and $R_{\rm HT}$ show clearly that the A_1^* is relatively more important in CEX than in diffractive production. Thus one should not be surprised that the introduction of 1^+ background does not significantly affect the ACCMOR results, but does have important effects in charge exchange.

It is highly likely that inclusion of (nondiffractive but still "Deck-type") multi-Regge background as

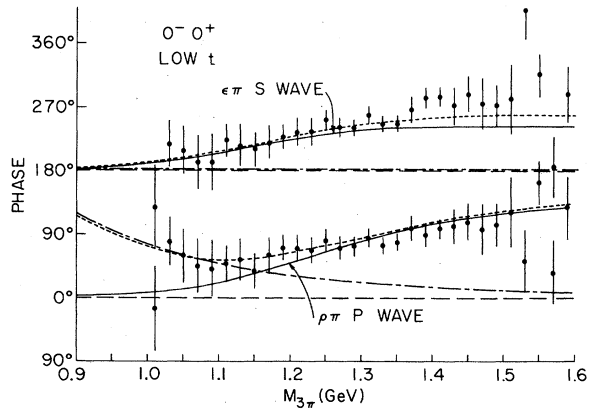

FIG. 4. LT, 0^-0^+ phases; labeling same as in Fig. 3.

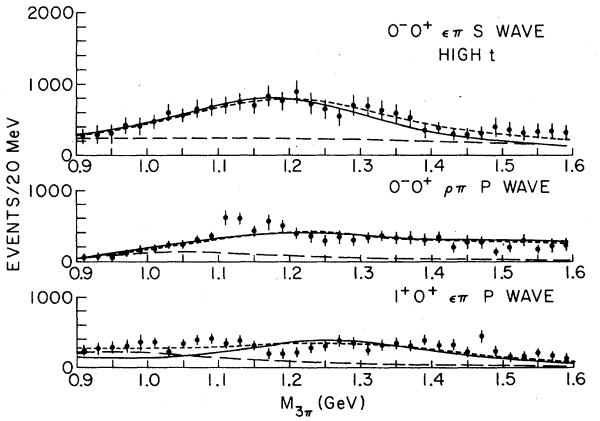

FIG. 6. HT, 1^+0^+ and 0^-0^+ $\rho\pi$ and $\epsilon\pi$ cross sections.

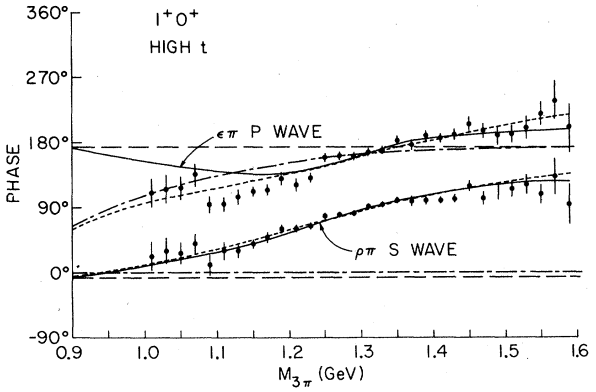

FIG. 7. HT, 1^+0^+ phases.

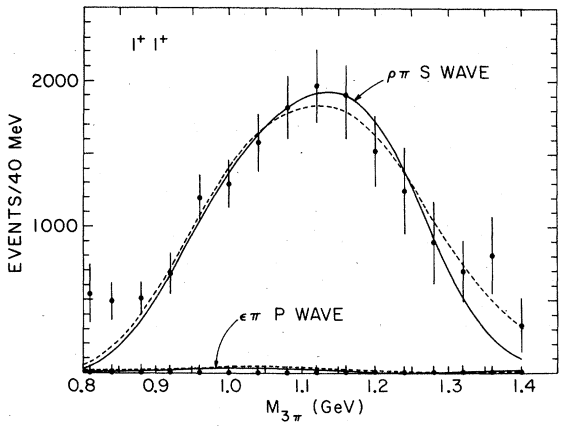

FIG. 9. CEX $\rho\pi$ and $\epsilon\pi$ cross sections.

done by the authors of Ref. 2 could equally well explain the CEX results. We would argue that their approach and ours are dual to one another, and not physically distinct.

(3) Rescattering at low energies. It is clear from Figs. 1–10 that our theory does a poor job of fitting the data at low energies (near $\rho\pi$ threshold). Our previous experience, fitting such low-energy data using a unitary three-body model, indicates that neglect of rescattering is responsible for the poor threshold performance of our present model.[6] While we now believe the former model to be somewhat untrustworthy,[11] we still feel that certain features of that model should be included in our present fitting procedure. For example, we found an anomalously large $J^P=1^+$ p-wave Deck amplitude produced by rescattering via the enormous s-wave Deck process, and furthermore, that this rescattering shifted the phase of the p-wave Deck amplitude by approximately 90° relative to the s-wave Deck amplitude.

Instead of systematically inserting rescattering diagrams into the present theory, we decided on a much simpler approach; namely, to modify our p-wave Deck to have a phase consistent with our previous results. We feel that the latter approach is legitimate for the Deck amplitudes because it represents inclusion of long-range rescattering (π exchange), and as such, is to large extent model independent (in the sense of a Watson-type final-state interaction factor). On the other hand, it is not a reasonable way to modify direct A_1 production where short-range interactions are important. In that case we hope that our phenomenological parametrization of the vertex V_{iP} is sufficiently rich to include rescattering effects. The phases of these modified Deck amplitudes and the corresponding cross sections are shown in Figs. 3–6. When the above phase behavior was included in our fitting procedure, the χ^2 dropped from 1214 to 778 without a substantial change in the A_1 and π' resonance parameters. The fits for this case are shown in Figs. 1–10. Thus we believe that the previously quoted χ^2 of 1214 was artificially high because of improper treatment of rescattering near threshold, and the χ^2 of 778 gives a fairer estimate of the quality of our fits. While we could assert the existence of a π' on the basis of the "without-

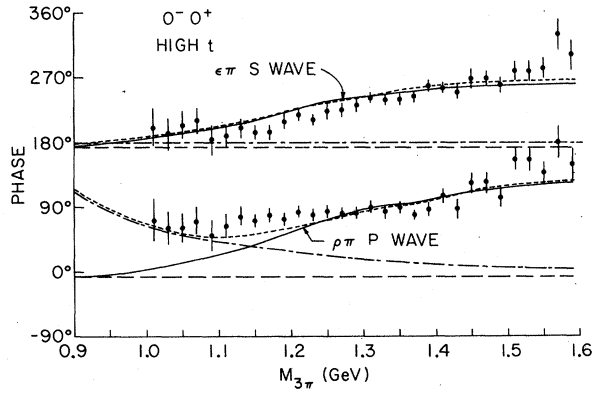

FIG. 8. HT, 0^-0^+ phases.

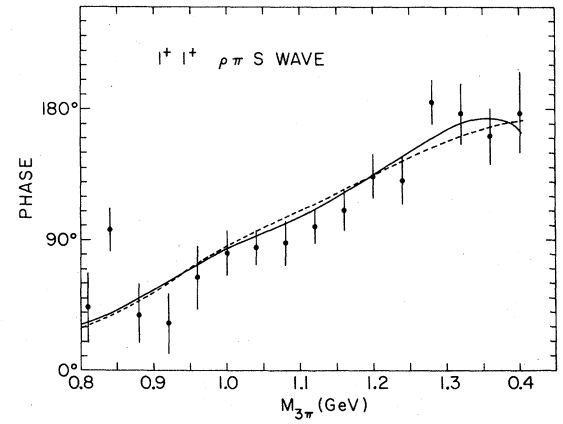

FIG. 10. CEX $\rho\pi$ phase.

TABLE I. Three-pion resonance parameters (MeV).

	Mass	$\Gamma_{\rho\pi}$	$\Gamma_{\epsilon\pi}$	Γ_{total}
$J^P=1^+$	1230 ± 30	336	14	350 ± 60
$J^P=0^-$	1273 ± 50	163	345	508 ± 100

rescattering" curves, our case is then much less convincing. We have already given theoretical support for the manner in which we have included rescattering. Additional justification is provided *a posteriori* by noting that neither the A_1 nor π' parameters are very sensitive to the rescattering. This result is presented in Table II where we display certain fitting parameters obtained with and without rescattering.

VI. DISCUSSION

In this paper we have fitted 1^+ and 0^- 3π results available from recent diffractive and charge-exchange experiments, using a generalized version of a model first suggested by Aitchison and Bowler.[3] This model incorporates in a unitary manner Deck background (nonresonant production) and resonance production. We assume that all resonant production proceeds through intermediate states obtained from quark-model calculations. In our particular fit we include two such states as suggested by bag-model calculations of Jaffe and collaborators. The presence of two fundamental quark states in the A_1 region is also suggested by previous phenomenological work of Basdevant and Berger.[12]

The connection between the discrete states of the quark model and the low-energy hadron states which actually appear can be very indirect. Nevertheless, in a recent publication, Jaffe and Low[13] point out a "reasonably precise" manner in which such connections can be made. In particular, the quark-model eigenstates are shown to be poles in a dynamical quantity called the P matrix. The P matrix in turn is simply related to the S matrix, and so may be extracted from measured phases and inelasticities.

TABLE II. Fitting parameters obtained with and without rescattering.

	Without rescattering	With rescattering
A_1 parameters		
$\gamma_{1\rho}$	0.95	0.98
$\gamma_{1\epsilon}$	0.70	0.87
$\gamma_{1\rho}/\gamma_{1\epsilon}$	1.36	1.13
$\gamma_{2\rho}$	2.52	2.02
$\gamma_{2\epsilon}$	4.34	4.13
$\gamma_{2\rho}/\gamma_{2\epsilon}$	0.58	0.49
M_1 (GeV)	1.11	1.09
M_2 (GeV)	3.81	3.55
π' parameters		
$\gamma_{1\rho}/\gamma_{1\epsilon}$	0.081	0.121
M_1 (GeV)	1.28	1.27

The A_1 can be considered a one-channel ($\rho\pi$) problem to good approximation because of its small width into $\epsilon\pi$. For such a case (according to Jaffe and Low) the poles of the P matrix are obtained from the poles of

$$k\cot[kb+\delta(k)], \tag{6.1}$$

where b is an effective "bag" radius, and $\delta(k)$ is the $\rho\pi$ scattering phase obtained from our fitting procedure. While there is only one $J^P=1^+$ S-matrix pole in the energy range of the data, there are two P-matrix poles. In Fig. 11(a) we plot the positions of these poles as a function of b by substituting the $\rho\pi$ phase shift obtained from our best fits into (6.1). The behavior of these P-matrix poles may be compared with the more familiar ones of $\pi\pi$ scattering shown in Fig. 11(b). For b

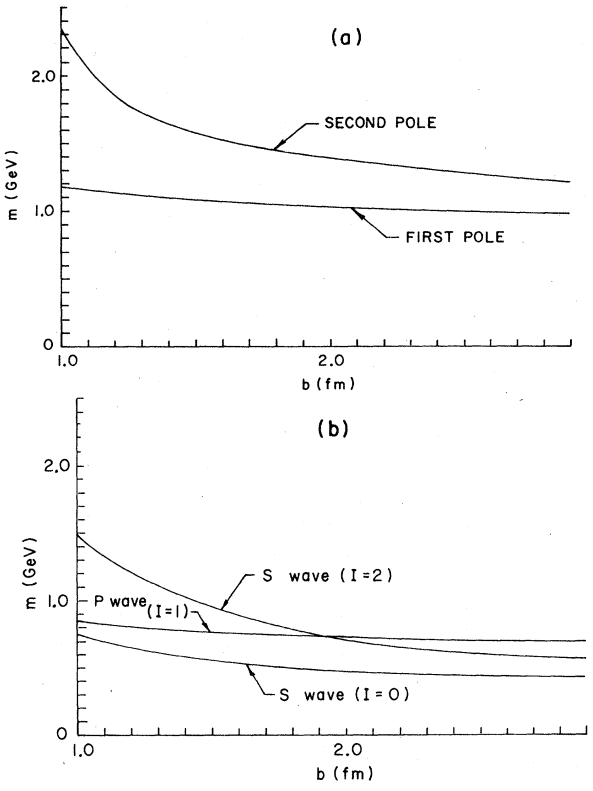

FIG. 11. (a) P-matrix poles in $J^P=1^+$ $\rho\pi$ system as function of bag radius. The results of Refs. 4 and 7 suggest that the first pole be interpreted as a $q\bar{q}$ state, and the second as a $q^2\bar{q}^2$ state. (b) P-matrix poles in $\pi\pi$ scattering vs bag radius.

$=1.6f$, the value used in the bag model for the $\pi\pi$ system, the P-matrix poles appear at ~1100 MeV and ~1450 MeV. According to Jaffe and Low, we should interpret these pole positions in terms of discrete states of the quark model. Tables IV and II of Refs. 7 and 4, respectively, suggest that we associate the lower-mass pole with a $q\bar{q}$ state, and the higher-mass pole with a $q^2\bar{q}^2$ state. Because the latter state has color-singlet subunits, it is expected to be wide and behave like a background.

The final picture which emerges from our analysis holds together very nicely. Our 0^- (π') is a new result, and this state is presumably a $q\bar{q}$ excited state. However, we believe that what is usually referred to as the A_1 can be qualitatively understood in terms of two quark-model states, $q\bar{q}$ (~1100) and $q^2\bar{q}^2$ (~1450). In fact, it is probably the presence of two such overlapping states that accounts in large part for the traditional difficulties involved in analyzing the 1^+ three-pion system in strong interaction experiments.

ACKNOWLEDGMENTS

The work of R. A. was supported in part by the National Science Foundation. The work of R. S. L. was supported by the U. S. Department of Energy under Contract No. DE-AC02-76CH00016.

APPENDIX A: MULTICHANNEL RESONANCE SCATTERING

We here obtain forms for the amplitudes $\bar{f}^R_a$ given in Eqs. (3.8) and (3.9) of the text. We begin by introducing auxiliary two-body amplitudes $t_{i,a\alpha}(W_A)$ for each member of the quark spectrum predicted by standard "confined" calculations. (Jaffe and Low[13] refer to such states as primitives.) Each primitive is labeled by the subscript i, and we permit initial states $\alpha=P,\rho,\epsilon$, and final states $a=\rho$ and ϵ. We assume that an isolated primitive gives rise to a *unitary* t matrix which, in operator formalism, may be written

$$t_{i,a\alpha}(W_A)=|ia\rangle D_{ii}^{-1}(W_A)\langle i\alpha|\,. \tag{A1}$$

We make contact with the vertex functions in the text by taking matrix elements of (A1), and defining

$$\begin{aligned}\langle p|i\alpha\rangle &= V_{i\alpha}(p) \quad \text{for } \alpha=P\\ &= u_{i\alpha}(p) \quad \text{for } \alpha=\rho,\epsilon\,.\end{aligned} \tag{A2}$$

In the vicinity of a narrow resonance, the inverse propagator D_{ii}^{-1} takes the form

$$D_{ii}(W_A)\cong M_A - W_A - i\Gamma_i(W_A)/2\,, \tag{A3}$$

where M_A is the resonant energy, and $\Gamma_i(M_A)$ is the total width. The simplest choice for $D_{ii}(W_A)$ which leads to a unitary set of $t_{i,a\alpha}$, and the one that we shall use in our fitting procedure, is that of (A3) with

$$\Gamma_i(W_A)=2[u_{i\epsilon}^2(p_A)+u_{i\rho}^2(p_A)]\,. \tag{A4}$$

In (A4) above, p_A is the relative momentum of the $\rho\pi$ ($\epsilon\pi$) system corresponding to total c.m. energy W_A.

We now consider the case of two quark-related resonances with considerable overlap—a situation that we believe corresponds most closely to the 3π system near 1 GeV. The amplitudes $\bar{f}^R_a$ given in Eqs. (3.8) and (3.9) may then be expressed formally as the following operator expansion (a diagrammatic representation is shown in Fig. 12):

$$\begin{aligned}\bar{f}^R_{a\alpha}(W_A)=&\sum_{i=1}^{2} t_{i,a\alpha}(W_A)\\ &+\sum_{\substack{i\neq j=1\\ b}}^{2} t_{i,ab}(W_A)G_b^{(0)}(W_A)t_{j,b\alpha}(W_A)+\cdots\,.\end{aligned} \tag{A5}$$

In (A5) the quantity $G_b^{(0)}$ is the free-particle πb propagator. Its precise form is not necessary for future discussion; we require only that the matrix element

$$D_{12}=\sum_a \langle 1a|G^{(0)}_{\alpha a}(W_A)|2a\rangle \tag{A6}$$

exists and is a smooth function of W_A.

We may now sum (A5) above using methods developed by Faddeev[14] for the nonrelativistic three-body problem. Suppressing the argument W_A, we write

$$\bar{f}^R_{a\alpha}=T^{(1)}_{a\alpha}+T^{(2)}_{a\alpha}\,, \tag{A7}$$

where

$$T^{(1)}_{a\alpha}=|1a\rangle D_{11}^{-1}\langle 1\alpha|+|1a\rangle D_{11}^{-1}\tau^{(1)}_\alpha\,, \tag{A8}$$

$$T^{(2)}_{a\alpha}=|2a\rangle D_{22}^{-1}\langle 2\alpha|+|2a\rangle D_{22}^{-1}\tau^{(2)}_\alpha\,, \tag{A9}$$

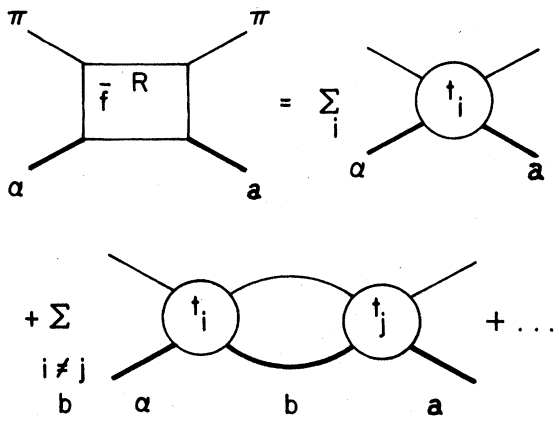

FIG. 12. Diagrammatic representation of $\bar{f}^R_{a\alpha}$.

with

$$\tau_\alpha^{(1)} = \sum_b \langle 1b | G_b^{(0)} T_{b\alpha}^{(2)}, \tag{A10}$$

$$\tau_\alpha^{(2)} = \sum_b \langle 2b | G_b^{(0)} T_{b\alpha}^{(1)}. \tag{A11}$$

One can check that (A7)–(A11) give a formally correct solution by iterating (A8) and (A9) in (A7) using (A10) and (A11), and recovering the expansion (A5).

Multiplying (A8) and (A9) by $\langle 2a | G_a^{(0)}$ and $\langle 1a | G_a^{(0)}$, respectively, and summing over a, we obtain the following set of linear algebraic equations for $\tau_\alpha^{(1)}$ and $\tau_\alpha^{(2)}$:

$$\tau_\alpha^{(2)} = D_{21} D_{11}^{-1} \langle 1\alpha | + D_{21} D_{11}^{-1} \tau_\alpha^{(1)}, \tag{A12}$$

$$\tau_\alpha^{(1)} = D_{12} D_{22}^{-1} \langle 2\alpha | + D_{12} D_{22}^{-1} \tau_\alpha^{(2)}, \tag{A13}$$

where

$$D_{21} = D_{12} = \sum_a \langle 1a | G_a^{(0)} | 2a \rangle. \tag{A14}$$

Finally, substituting (A12) and (A13) into (A8) and (A9), we obtain for (A7)

$$\bar{f}_{a\alpha}^R = \sum_{i,j=1}^{2} |ja\rangle D_{\tilde{i}\tilde{j}} \langle i\alpha | / |\det D|, \tag{A15}$$

where $\tilde{i}$ and $\tilde{j}$ are defined such that if $i=1$, then $\tilde{i}=2$, and vice versa.

In our fitting procedure we choose $D_{12}(W_A)$ to be

$$D_{12}(W_A) = i[u_{1\rho}(p_A) u_{2\rho}(p_A) + u_{1\epsilon}(p_A) u_{2\epsilon}(p_A)]. \tag{A16}$$

Simple models indicate that such a choice is reasonable. With D_{ij} given by (A3), (A4), and (A16), it is shown in Appendix B that the t-matrix formalism developed in this Appendix (for two overlapping resonances) is equivalent to a standard two-pole K-matrix model. Thus, our formalism is neither more nor less justified than the usual K-matrix approach; however, our prejudice is that the t-matrix parametrization that we use gives more physical insight into the problem at hand, while offering a more general unitary and analytic framework for future application.[15] For example, we obtain the model of Aitchison and Bowler,[3] if rather than the simple resonance form (A3), we choose $D_{ij}(W_A)$ to satisfy a dispersion relation

$$D_{ij}(W_A) = A + BW_A + \frac{1}{\pi} \int_{x_0}^{\infty} dx \frac{\mathrm{Im} D_{ij}(W_A)}{x - W_A - i\epsilon}. \tag{A17}$$

APPENDIX B: K-MATRIX FORMALISM

In this appendix we show that for a single channel (e.g., $\rho\pi$) and two intermediate resonances, the formalism developed in the previous Appendix, as applied in the text, is equivalent to a standard two-pole K-matrix model. The extension of this result to the multichannel situation is tedious but straightforward, and shall not be discussed here.

Consistent with the material in Appendix A and the main text, we write schematically for one channel and two resonances

$$\bar{f}^R = \frac{u_1 D_{22} u_1 + u_2 D_{11} u_2 + 2u_1 D_{12} u_2}{D_{11} D_{22} - D_{12}^2}, \tag{B1}$$

where

$$\begin{aligned} D_{11} &= M_1 - W - i\Gamma_1/2, \\ D_{22} &= M_2 - W - i\Gamma_2/2, \\ D_{12} &= D_{21} = i(\Gamma_1\Gamma_2/4)^{1/2}, \end{aligned} \tag{B2}$$

and

$$\begin{aligned} u_1 &= (\Gamma_1/2)^{1/2}, \\ u_2 &= (\Gamma_2/2)^{1/2}. \end{aligned} \tag{B3}$$

Substituting (B2) and (B3) into (B1), we obtain

$$\bar{f}^R = \frac{(M_2 - W)\Gamma_1/2 + (M_1 - W)\Gamma_2/2}{(M_1 - W)(M_2 - W) + i[(M_2 - W)\Gamma_1/2 + (M_1 - W)\Gamma_2/2]}. \tag{B4}$$

To compare with the standard K-matrix formalism we define, as in Sec. III,

$$\begin{aligned} q\gamma_1^2 &= \Gamma_1/2, \\ q\gamma_2^2 &= \Gamma_2/2. \end{aligned} \tag{B5}$$

Equation (B4) may now be rewritten

$$\bar{f}^R = \frac{q}{K^{-1} - iq}, \tag{B6}$$

where

$$K = \sum_{i=1}^{2} \frac{\gamma_i^2}{M_i - W}. \tag{B7}$$

The above equation is the standard K-matrix assumption.

---

[1] Amsterdam–CERN–Crakow–Munich–Oxford–Rutherford Collaboration (hereafter referred to as ACCMOR), Phys. Lett. 89B, 281 (1980). This reference contains only the 1^+ $\rho\pi$ data. The 1^+ $\epsilon\pi$ and 0^- $\rho\pi$ diffractive data were provided by the ACCMOR collaboration (private communication).

[2] Carleton–McGill–Ohio State–Toronto Collaboration (hereafter referred to as CEX for charge exchange), J. A. Dankowych *et al.*, Phys. Rev. Lett. 46, 580 (1981).

[3]M. G. Bowler, M. A. V. Game, I. J. R. Aitchison, and J. B. Dainton, Nucl. Phys. B97, 227 (1975).
[4]R. J. Jaffe, Phys. Rev. D 15, 267 (1977).
[5]D. J. Herndon, P. Soding, and R. J. Cashmore, Phys. Rev. D 11, 3165 (1975) (see p. 3176).
[6]R. Aaron, R. S. Longacre, and J. E. Sacco, Ann. Phys. (N.Y.) 117, 56 (1979).
[7]T. A. DeGrand and R. L. Jaffe, Ann. Phys. (N.Y.) 100, 425 (1976).
[8]The Deck background mechanism was first discussed by R. T. Deck, Phys. Rev. Lett. 13, 169 (1964). A description of the parametrization of such background amplitudes for input in partial-wave analyses of the 3π system may be found, for example, in M. G. Bowler and M. A. V. Game, Oxford University Report No. ONP 38/74 (unpublished).
[9]See, for example, the Appendix of Ref. 6.
[10]R. Aaron and R. D. Amado, Phys. Rev. Lett. 31, 1157 (1973).
[11]In the analysis of Ref. 6, the A_1 appears at ~1500 MeV, an energy which we now know is too large. This incorrect result was obtained partly because we assumed that the 0^- $\epsilon\pi$ amplitude had small phase variation, and used it as a reference wave. In fact, as shown in this present work, there is a 0^- resonance at ~1280 MeV. However, the above mentioned difficulty is not the only problem. Subsequent work with the Q-meson systems indicated that the amplitudes of Ref. 6 have inherently bad off-shell behavior in the presence of large Deck contributions. This behavior is presumably due to the approximations required to solve the relevant relativistic three-body equations.
[12]J. L. Basdevant and E. L. Berger, Phys. Rev. D 16, 657 (1977). Their best fit to the data (solution E) contains "two poles." We interpret these two poles as reflections of the two quark-related states referred to in the text.
[13]R. L. Jaffe and F. E. Low, Phys. Rev. D 19, 2105 (1979).
[14]L. D. Faddeev, Zh. Eksp. Teor. Fiz. 39, 1459 (1960) [Sov. Phys.—JETP 12, 1014 (1961)]; *Mathematical Aspects of the Three-Body Problem* (Davey, New York, 1965).
[15]A similar model has been used by R. E. Cutkosky and R. L. Kelly in their ongoing analysis of πN data. [See, for example, R. E. Cutkosky, contribution to the IV International Conference on Baryon Resonances, Toronto, 1980 (unpublished)].